Journal of King Saud University – Science 33 (2021) 101244

Contents lists available at ScienceDirect

Journal of King Saud University – Science

journal homepage: www.sciencedirect.com

Original article

Numerical solutions of two-dimensional nonlinear fractional Volterra and Fredholm integral equations using shifted Jacobi operational matrices via collocation method

Jalil Rashidinia *, Tahereh Eftekhari, Khosrow Maleknejad

School of Mathematics, Iran University of Science & Technology (IUST), Narmak, Tehran 16846 13114, Iran

ARTICLE INFO

Article history:
Received 2 September 2020
Revised 28 October 2020
Accepted 31 October 2020
Available online 23 November 2020

Keywords:
Two-dimensional nonlinear fractional Volterra and Fredholm integral equations
Two-variable shifted Jacobi polynomials
Collocation method
Operational matrices
Convergence analysis

ABSTRACT

In this paper, an efficient numerical method is presented to approximate solutions of two-dimensional nonlinear fractional Volterra and Fredholm integral equations. We derive new operational matrices of fractional-order integration and product based on two-variable shifted Jacobi polynomials. These operational matrices via shifted Jacobi collocation method are utilized to reduce the understudy equations to systems of linear or nonlinear algebraic equations. Then, the arising systems can be solved by the Newton method. Discussion on the error bound and convergence analysis of the proposed method is presented. The efficiency, accuracy, and validity of the presented method are demonstrated by its application to three test examples and by comparing our results with the results obtained by existing methods in the literature.

1. Introduction

Fractional calculus is the generalization of calculus, in which the order of derivatives and integrals can be arbitrary numbers. The history of fractional calculus is more than three centuries old; however, only in the last two decades, the field has received practical attention and interest. Many researchers have shown with the applications of fractional calculus to groundwater flow problems and groundwater pollution (Atangana and Kılıçman, 2013a; Benson et al., 2000; Caputo, 1967; Cloot and Botha, 2006; Meerschaert and Tadjeran, 2004), acoustic wave problems (Atangana and Kılıçman, 2013b), and others (Chen et al., 2007; Mainardi, 1997; Yuste and Acedo, 2005; Zhuang et al., 2009). Moreover, advances in sciences have led to the formation of many physical and engineering problems that can be mathematically represented by fractional integro-differential equations (FIDEs). For example, problems from rheology, porous media, electrochemistry, control, electromagnetism fluid structure, viscoelasticity, coupling and particle mechanics (see e.g. Carpinteri and Mainardi, 1997; Metzler et al., 1995; Oldham and Spanier, 1974; Thomas and Fehmi, 2010). In recent years, numerical methods for solving FIDEs have attracted the attention of a large number of researchers. Such as, Ma and Huang (2013) have proposed a hybrid collocation method for solving FIDEs. Mohammed (2014) has developed an approximate scheme based on least squares method with aid of shifted Chebyshev polynomial to solve linear FIDEs. Alkan (2015) has obtained numerical solutions of a class of nonlinear Fredholm FIDEs by using sinc–collocation method. Maleknejad et al. (2020a) have proposed operational matrix method based on the hybrid of two-dimensional block-pulse functions and two-variable shifted Legendre polynomials (2D-HBPSLs) to solve nonlinear two-dimensional FIDEs of the general form. Nemati et al. (2020) have presented a collocation method based on the Legendre wavelet combined with the Gauss-Jacobi quadrature formula for calculating the numerical solution of a class of delay-type FIDEs. For a review on numerical techniques, proposed to solve other different problems, see for instance Kumar et al., 2017, 2018, 2020, Maleknejad et al., 2018, 2021; Mirzaee et al., 2018; Mirzaee and Alipour, 2018, 2019a, 2019b, Mirzaee and

* Corresponding author.
E-mail addresses: rashidinia@iust.ac.ir (J. Rashidinia), t.eftekhari2009@gmail.com (T. Eftekhari), maleknejad@iust.ac.ir (K. Maleknejad).

Peer review under responsibility of King Saud University.

Production and hosting by Elsevier

https://doi.org/10.1016/j.jksus.2020.101244

Samadyar, 2018a, 2018b; Samadyar and Mirzaee, 2019; Singh, 2020a, 2020b, Singh et al., 2019, 2020; Singh and Srivastava, 2020; Yadav et al., 2019 and references therein.

In this paper, the following fractional integral equations of the second kind are considered:

Two-dimensional nonlinear fractional Volterra integral Eqs. (2D-NFVIEs):

$$f(x,y)=g(x,y)+\frac{1}{\Gamma(\imath_1)\Gamma(\imath_2)}\int_0^x\int_0^y(x-\tau)^{\imath_1-1}(y-\varsigma)^{\imath_2-1}k(x,y,\tau,\varsigma)f^p(\tau,\varsigma)\,d\varsigma\,d\tau, \tag{1}$$

Two-dimensional nonlinear fractional Fredholm integral Eqs. (2D-NFFIEs):

$$f(x,y)=g(x,y)+\frac{1}{\Gamma(\imath_1)\Gamma(\imath_2)}\int_0^{\ell_1}\int_0^{\ell_2}(\ell_1-\tau)^{\imath_1-1}(\ell_2-\varsigma)^{\imath_2-1}\times k(x,y,\tau,\varsigma)f^p(\tau,\varsigma)\,d\varsigma\,d\tau, \tag{2}$$

where $f(x,y)$ is an unknown function and $g(x,y), k(x,y,\tau,\varsigma)$ are given functions. Also, $\imath_1,\imath_2>0$ and $(x,y)\in\Omega=[0,\ell_1]\times[0,\ell_2]$.

Najafalizadeh and Ezzati (2016) constructed operational matrices of fractional-order integration and product for two-dimensional block pulse functions (2D-BPFs) and applied them to solve Eqs. (1) and (2). Jabari Sabeg et al. (2017) derived the operational matrix of two-dimensional orthogonal triangular functions (2D-TFs) for two-dimensional fractional integrals. Then, they applied this operational matrix and properties of two-dimensional orthogonal triangular functions to solve Eq. (1). Hesameddini and Shahbazi (2018) used the operational matrix method based on two-dimensional shifted Legendre polynomials (2D-SLPOM) for the numerical solution of Eqs. (1) and (2). Mirzaee and Samadyar (2019) developed a numerical scheme based on two-dimensional orthonormal Bernstein polynomials (2D-OBPs) for solving Eqs. (1) and (2). Maleknejad et al. (2020b) have provided sufficient conditions for the local and global existence of solutions for Eqs. (1) and (2), based on the Schauder's and Tychonoff's fixed-point theorems. Also, they have provided sufficient conditions for the uniqueness of the solutions. Moreover, they have used operational matrix method based on the 2D-HBPSLs via collocation method to find approximate solutions of the mentioned equations in a Banach space. Moreover, Maleknejad et al., 2020 applied a new and efficient numerical method based on shifted fractional-order Jacobi operational matrices for solving Eqs. (1) and (2). In this research study, we present an efficient numerical method, based on two-variable shifted Jacobi polynomials (SJPs), to approximate the solutions of (1) and (2) using operational matrices of fractional-order integration and product via shifted Jacobi collocation method. The main advantage of the proposed technique is that the problems under consideration are reduced to systems of linear or nonlinear algebraic equations. Then, the arising systems can be solved by the Newton method.

The outline of this paper is organized as follows. In Section 2, a review of fractional calculus and also one-variable SJPs is given. In Section 3, we introduce two-variable SJPs and then we derive operational matrices of fractional-order integration and product based on these polynomials. In Section 4, we explain the numerical solutions of 2D-NFVIEs and 2D-NFFIEs, respectively, by using what was introduced in Section 3. Also, in Section 5, the error bound and convergence analysis of the presented method are studied. Moreover, three test examples are given in Section 6 to demonstrate the effectiveness of the method. Finally, a conclusion is given in Section 7.

2. Preliminary knowledge

2.1. Fractional calculus

Definition 1 (*Podlubony, 1999*). The Riemann–Liouville fractional integral of order $\alpha>0$ is defined by

$$I^\alpha f(x)=\frac{1}{\Gamma(\alpha)}\int_0^x(x-\tau)^{\alpha-1}f(\tau)\,d\tau,$$

where $\Gamma(.)$ is the gamma function.

Definition 2. (*Abbas and Benchohra, 2014*). The left-sided mixed Riemann–Liouville integral of order $\imath=(\imath_1,\imath_2)\in(0,\infty)\times(0,\infty)$ of f is defined by

$$I^\imath f(x,y)=\frac{1}{\Gamma(\imath_1)\Gamma(\imath_2)}\int_0^x\int_0^y(x-\tau)^{\imath_1-1}(y-\varsigma)^{\imath_2-1}f(\tau,\varsigma)\,d\varsigma\,d\tau.$$

2.2. One-variable SJPs and their properties

The one-variable SJPs are defined on the interval $[0,\ell]$ by

$$\mathscr{J}_{\ell,k}^{(\varrho,\vartheta)}(x)=\sum_{j=0}^{k}(-1)^{k-j}\frac{\Gamma(k+\vartheta+1)\Gamma(k+j+\varrho+\vartheta+1)}{\Gamma(j+\vartheta+1)\Gamma(k+\varrho+\vartheta+1)(k-j)!j!\ell^j}x^j,$$

with the following orthogonality property on the interval $[0,\ell]$:

$$\int_0^\ell \mathscr{J}_{\ell,i}^{(\varrho,\vartheta)}(x)\mathscr{J}_{\ell,i'}^{(\varrho,\vartheta)}(x)w_\ell^{(\varrho,\vartheta)}(x)\,dx=h_{\ell,i}^{(\varrho,\vartheta)}\delta_{ii'},$$

where $\delta_{ii'}$ is Kronecker delta, $w_\ell^{(\varrho,\vartheta)}(x)=x^\vartheta(\ell-x)^\varrho$ is weight function, and

$$h_{\ell,k}^{(\varrho,\vartheta)}=\frac{\ell^{\varrho+\vartheta+1}\Gamma(k+\varrho+1)\Gamma(k+\vartheta+1)}{(2k+\varrho+\vartheta+1)k!\Gamma(k+\varrho+\vartheta+1)}.$$

Another property of one-variable SJPs is as follows:

$$\frac{d^i}{dx^i}\mathscr{J}_{\ell,k}^{(\varrho,\vartheta)}(x)=\frac{\Gamma(k+\varrho+\vartheta+i+1)}{\Gamma(k+\varrho+\vartheta+1)}\mathscr{J}_{\ell,k-i}^{(\varrho+i,\vartheta+i)}(x). \tag{3}$$

The vector of one-variable SJPs is in the following form:

$$\phi(x)=\left(\mathscr{J}_{\ell,0}^{(\varrho,\vartheta)}(x)\quad \mathscr{J}_{\ell,1}^{(\varrho,\vartheta)}(x)\quad\ldots\quad \mathscr{J}_{\ell,N}^{(\varrho,\vartheta)}(x)\right)^T. \tag{4}$$

3. Two-variable SJPs and their operational matrices of fractional-order integration and product

3.1. Two-variable SJPs and function approximation

The two-variable SJPs are defined on the domain $\Omega=[0,\ell_1]\times[0,\ell_2]$ by

$$\mathscr{J}_{i,j}^{(\varrho,\vartheta)}(x,y)=\mathscr{J}_{\ell_1,i}^{(\varrho,\vartheta)}(x)\mathscr{J}_{\ell_2,j}^{(\varrho,\vartheta)}(y),$$

for i, j = 0,1,2,...,N, with the following orthogonality property on the domain Ω:

$$\int_0^{\ell_1}\int_0^{\ell_2}\mathscr{J}_{i,j}^{(\varrho,\vartheta)}(x,y)\mathscr{J}_{i',j'}^{(\varrho,\vartheta)}(x,y)\omega^{(\varrho,\vartheta)}(x,y)\,dy\,dx=h_{\ell_1,i}^{(\varrho,\vartheta)}h_{\ell_2,j}^{(\varrho,\vartheta)}\delta_{ii'}\delta_{jj'},$$

where $\omega^{(\varrho,\vartheta)}(x,y)=w_{\ell_1}^{(\varrho,\vartheta)}(x)w_{\ell_2}^{(\varrho,\vartheta)}(y)$ is weight function.

A two-variable continuous function $f(x,y)$ in the domain $\Omega=[0,\ell_1]\times[0,\ell_2]$ can be approximated by using the two-variable SJPs as follows:

$$f(x,y)\simeq f_N(x,y)=\sum_{i=0}^{N}\sum_{j=0}^{N}\hat{f}_{ij}\mathscr{J}_{i,j}^{(\varrho,\vartheta)}(x,y)=\Phi^T(x,y)\hat{F}=\hat{F}^T\Phi(x,y), \quad (5)$$

where $\hat{F}$ is an $(N+1)^2\times 1$ vector of unknown coefficients as:

$$\hat{F}=\left(\hat{f}_{00},\hat{f}_{01},\dots\hat{f}_{0N},\hat{f}_{10},\hat{f}_{11},\dots,\hat{f}_{1N},\dots,\hat{f}_{N0},\hat{f}_{N1},\dots,\hat{f}_{NN}\right)^T,$$

with entries

$$\hat{f}_{ij}=\frac{1}{h_{\ell_1,i}^{(\varrho,\vartheta)}h_{\ell_2,j}^{(\varrho,\vartheta)}}\int_0^{\ell_1}\int_0^{\ell_2}f(x,y)\mathscr{J}_{i,j}^{(\varrho,\vartheta)}(x,y)\omega^{(\varrho,\vartheta)}(x,y)\,\mathrm{d}y\,\mathrm{d}x,$$

for i,j = 0,1,…,N. Also $\Phi(x,y)$ is an $(N+1)^2\times 1$ vector of two-variable SJPs as:

$$\Phi(x,y)=(\mathscr{J}_{0,0}^{(\varrho,\vartheta)}(x,y),\dots,\mathscr{J}_{0,N}^{(\varrho,\vartheta)}(x,y),\mathscr{J}_{1,0}^{(\varrho,\vartheta)}(x,y),\dots,\mathscr{J}_{1,N}^{(\varrho,\vartheta)}(x,y),\dots,\mathscr{J}_{N,0}^{(\varrho,\vartheta)}(x,y),\dots,\mathscr{J}_{N,N}^{(\varrho,\vartheta)}(x,y))^T. \quad (6)$$

Let $k(x,y,\tau,\varsigma)$ be a function of four variables in $\Omega\times\Omega$. It can be similarly expanded with respect to two-variable SJPs as

$$k(x,y,\tau,\varsigma)\simeq\Phi^T(x,y)K\Phi(\tau,\varsigma), \quad (7)$$

where K is an $(N+1)^2\times(N+1)^2$ matrix with entries

$$K_{i,j}=\int_0^{\ell_1}\int_0^{\ell_2}\int_0^{\ell_1}\int_0^{\ell_2}\left(\mathscr{J}_{p[i],q[i]}^{(\varrho,\vartheta)}(x,y)k(x,y,\tau,\varsigma)\mathscr{J}_{p[j],q[j]}^{(\varrho,\vartheta)}(\tau,\varsigma)\times\omega^{(\varrho,\vartheta)}(x,y)\omega^{(\varrho,\vartheta)}(\tau,\varsigma)\,\mathrm{d}\varsigma\,\mathrm{d}\tau\,\mathrm{d}y\,\mathrm{d}x\right)/\left(h_{\ell_1,p[i]}^{(\varrho,\vartheta)}h_{\ell_2,q[i]}^{(\varrho,\vartheta)}h_{\ell_1,p[j]}^{(\varrho,\vartheta)}h_{\ell_2,q[j]}^{(\varrho,\vartheta)}\right),$$

for $i,j=1,2,\dots,(N+1)^2$, and

$$p=[0,0,\dots,0,1,1,\dots,1,\dots,N,N,\dots,N],$$
$$q=[0,1,\dots,N,0,1,\dots,N,\dots,0,1,\dots,N],$$

are two vectors of indices.

3.2. Operational matrices of fractional-order integration

Khalil and Khan (2014) defined an $(N+1)\times(N+1)$ operational matrix of one-dimensional integration of fractional order α in the Riemann–Liouville sense by

$$\mathbf{I}^{\ell,\alpha}=\begin{pmatrix}S_{00}&S_{01}&\dots&S_{0N}\\S_{10}&S_{11}&\dots&S_{1N}\\\vdots&\vdots&\ddots&\vdots\\S_{N0}&S_{N1}&\dots&S_{NN}\end{pmatrix},$$

with the entries

$$S_{nl}=\sum_{j=0}^{n}\left(\frac{(-1)^{n-j}\Gamma(n+\vartheta+1)\Gamma(n+j+\varrho+\vartheta+1)\Gamma(j+1)}{\Gamma(j+\vartheta+1)\Gamma(n+\varrho+\vartheta+1)(n-j)!j!\Gamma(j+\alpha+1)\ell^j}\times\sum_{i=0}^{l}\frac{(-1)^{l-i}(2l+\varrho+\vartheta+1)\Gamma(l+1)\Gamma(l+i+\varrho+\vartheta+1)\Gamma(j+\alpha+i+\vartheta+1)\Gamma(\alpha+1)\ell^\alpha}{\Gamma(l+\varrho+1)\Gamma(i+\vartheta+1)(l-i)!i!\Gamma(j+\alpha+i+\vartheta+\varrho+2)}\right),$$

where $n,l=0,1,2,\dots,N$.

Theorem 1. *Let $\iota:=(\iota_1,\iota_2)\in(0,\infty)\times(0,\infty)$, and $\Phi(x,y)$ be the vector of two-variable SJPs defined in (6). Then*

$$I^\iota\Phi(x,y)\simeq\left(\mathbf{I}^{\ell_1,\iota_1}\otimes\mathbf{I}^{\ell_2,\iota_2}\right)\Phi(x,y), \quad (8)$$

where $\mathbf{I}^{\ell_1,\iota_1}$ and $\mathbf{I}^{\ell_2,\iota_2}$ are $(N+1)\times(N+1)$ operational matrices of one-dimensional integration of fractional orders ι_1 and ι_2, respectively, in the Riemann–Liouville sense.

Proof. Since $\Phi(x,y)=\phi(x)\otimes\phi(y)$, we have

$$\begin{aligned}I^\iota\Phi(x,y)&=\tfrac{1}{\Gamma(\iota_1)\Gamma(\iota_2)}\int_0^x\int_0^y(x-\tau)^{\iota_1-1}(y-\varsigma)^{\iota_2-1}\Phi(\tau,\varsigma)\,d\varsigma\,d\tau\\&=\tfrac{1}{\Gamma(\iota_1)\Gamma(\iota_2)}\int_0^x\int_0^y(x-\tau)^{\iota_1-1}(y-\varsigma)^{\iota_2-1}(\phi(\tau)\otimes\phi(\varsigma))\,\mathrm{d}\varsigma\,\mathrm{d}\tau\\&=\left(\tfrac{1}{\Gamma(\iota_1)}\int_0^x(x-\tau)^{\iota_1-1}\phi(\tau)\,\mathrm{d}\tau\right)\otimes\left(\tfrac{1}{\Gamma(\iota_2)}\int_0^y(y-\varsigma)^{\iota_2-1}\phi(\varsigma)\,\mathrm{d}\varsigma\right)\\&=I^{\iota_1}\phi(x)\otimes I^{\iota_2}\phi(y)\\&\simeq\mathbf{I}^{\ell_1,\iota_1}\phi(x)\otimes\mathbf{I}^{\ell_2,\iota_2}\phi(y)\\&=\left(\mathbf{I}^{\ell_1,\iota_1}\otimes\mathbf{I}^{\ell_2,\iota_2}\right)(\phi(x)\otimes\phi(y))\\&=\left(\mathbf{I}^{\ell_1,\iota_1}\otimes\mathbf{I}^{\ell_2,\iota_2}\right)\Phi(x,y).\quad\square\end{aligned}$$

Theorem 2. *Let $\iota_1,\iota_2>0$. Suppose that $\Phi(\tau,\varsigma)$ is the vector of two-variable SJPs defined in (6). Then, we have*

$$\frac{1}{\Gamma(\iota_1)\Gamma(\iota_2)}\int_0^{\ell_1}\int_0^{\ell_2}(\ell_1-\tau)^{\iota_1-1}(\ell_2-\varsigma)^{\iota_2-1}\Phi(\tau,\varsigma)\,\mathrm{d}\varsigma\,\mathrm{d}\tau=Y_1\otimes Y_2, \quad (9)$$

where

$$Y_1=(\gamma1_0\quad\gamma1_1\quad\dots\quad\gamma1_N)^T,$$
$$Y_2=(\gamma2_0\quad\gamma2_1\quad\dots\quad\gamma2_N)^T,$$

and

$$\gamma1_k=\sum_{j=0}^{k}(-1)^{k-j}\frac{\Gamma(k+\vartheta+1)\Gamma(k+j+\varrho+\vartheta+1)\ell_1^{\iota_1}}{\Gamma(j+\vartheta+1)\Gamma(k+\varrho+\vartheta+1)(k-j)!\Gamma(j+\iota_1+1)},$$

$$\gamma2_k=\sum_{j=0}^{k}(-1)^{k-j}\frac{\Gamma(k+\vartheta+1)\Gamma(k+j+\varrho+\vartheta+1)\ell_2^{\iota_2}}{\Gamma(j+\vartheta+1)\Gamma(k+\varrho+\vartheta+1)(k-j)!\Gamma(j+\iota_2+1)},$$

for $k=0,1,\dots,N$.

Proof. From the definition of one-variable SJPs, we have

$$\begin{aligned}\gamma i_k&=\tfrac{1}{\Gamma(\iota_i)}\int_0^{\ell_i}(\ell_i-\varsigma)^{\iota_i-1}\mathscr{J}_{\ell_i,k}^{(\varrho,\vartheta)}(\varsigma)\mathrm{d}\varsigma\\&=\sum_{j=0}^{k}(-1)^{k-j}\frac{\Gamma(k+\vartheta+1)\Gamma(k+j+\varrho+\vartheta+1)}{\Gamma(j+\vartheta+1)\Gamma(k+\varrho+\vartheta+1)(k-j)!j!\ell_i^j}\left(\tfrac{1}{\Gamma(\iota_i)}\int_0^{\ell_i}(\ell_i-\varsigma)^{\iota_i-1}\varsigma^j\mathrm{d}\varsigma\right).\end{aligned}\quad(10)$$

for i = 1,2.

Let $s=\ell_i-\varsigma$. Therefore, we obtain

$$\frac{1}{\Gamma(\iota_i)}\int_0^{\ell_i}(\ell_i-\varsigma)^{\iota_i-1}\varsigma^j\,\mathrm{d}\varsigma=\frac{1}{\Gamma(\iota_i)}\int_0^{\ell_i}s^{\iota_i-1}(\ell_i-s)^j\,\mathrm{d}s.$$

Now with the change of variable $z=\frac{s}{\ell_i}$, we get

$$\begin{aligned}\tfrac{1}{\Gamma(\iota_i)}\int_0^{\ell_i}(\ell_i-\varsigma)^{\iota_i-1}\varsigma^j\mathrm{d}\varsigma&=\tfrac{\ell_i^{\iota_i+j-1}}{\Gamma(\iota_i)}\int_0^1z^{\iota_i-1}(1-z)^j\,\mathrm{d}z\\&=\tfrac{\ell_i^{\iota_i+j-1}}{\Gamma(\iota_i)}B(\iota_i,j+1)\\&=\ell_i^{\iota_i+j-1}\tfrac{\Gamma(j+1)}{\Gamma(j+\iota_i+1)},\end{aligned}$$

where $B(.,.)$ is Beta function. By substituting the above relation into (10), simplifying the obtained result, and using the relation $\Phi(\tau,\varsigma)$ =$\phi(\tau)\otimes\phi(\varsigma)$, we obtain Eq. (9). Therefore, the proof is completed. □

3.3. Operational matrix of product

Let $\Phi(x,y)$ be the vector of two-variable SJPs defined in (6). Borhanifar and Sadri (2016) obtained the operational matrix of product for $(x,y)\in[0,1]\times[0,1]$. In a similar way, we can compute this operational matrix for $(x,y)\in[0,\ell_1]\times[0,\ell_2]$ as follows:

$$\Phi(x,y)\Phi^T(x,y)\hat{F}\simeq\tilde{\hat{F}}\Phi(x,y), \quad (11)$$

where $\tilde{\hat{F}}$ is $(N+1)^2 \times (N+1)^2$ operational matrix of product with entries

$$\tilde{\hat{F}}_{m_1(N+1)+n_1+1, m_2(N+1)+n_2+1} = \frac{1}{h^{(\varrho,\vartheta)}_{\ell_1,m_2} h^{(\varrho,\vartheta)}_{\ell_2,n_2}} \sum_{j=0}^{N}\sum_{k=0}^{N} \hat{f}_{jk}\, v_{m_1jm_2}\, v_{n_1kn_2},$$

for $m_1, n_1, m_2, n_2 = 0, 1, \ldots, N$, and

$$v_{m_1jm_2} = \int_0^{\ell_1} \mathscr{J}^{(\varrho,\vartheta)}_{\ell_1,m_1}(x)\mathscr{J}^{(\varrho,\vartheta)}_{\ell_1 j}(x)\mathscr{J}^{(\varrho,\vartheta)}_{\ell_1,m_2}(x)w^{(\varrho,\vartheta)}_{\ell_1}(x)\,dx,$$
$$v_{n_1kn_2} = \int_0^{\ell_2} \mathscr{J}^{(\varrho,\vartheta)}_{\ell_2,n_1}(y)\mathscr{J}^{(\varrho,\vartheta)}_{\ell_2,k}(y)\mathscr{J}^{(\varrho,\vartheta)}_{\ell_2,n_2}(y)w^{(\varrho,\vartheta)}_{\ell_2}(y)\,dy.$$

4. The method of solution

In this section, we use two-variable SJPs and their operational matrices for solving Eqs. (1) and (2).

4.1. The method for 2D-NFVIEs

Here, we are going to convert Eq. (1) to a nonlinear system by using two-variable SJPs. First, we can write

$$g(x,y) \simeq \Phi^T(x,y)G, \tag{12}$$

By using (5) and (11) for the function $f(x,y)$, we obtain

$$[f(x,y)]^2 \simeq \hat{F}^T\Phi(x,y)\Phi^T(x,y)\hat{F} = \underbrace{\hat{F}^T\tilde{\hat{F}}}_{\hat{F}_2}\Phi(x,y) = \hat{F}_2\Phi(x,y),$$

$$[f(x,y)]^3 \simeq \hat{F}^T\Phi(x,y)\hat{F}_2\Phi(x,y) = \hat{F}^T\Phi(x,y)\Phi^T(x,y)\hat{F}_2^T = \underbrace{\hat{F}^T\tilde{\hat{F}}_2^T}_{\hat{F}_3}\Phi(x,y) = \hat{F}_3\Phi(x,y),$$

where $\tilde{\hat{F}}_2^T$ is an $N^2M^2 \times N^2M^2$ operational matrix of product. By continuing this process for an arbitrary $p \in \mathbb{N}$, we can write

$$[f(x,y)]^p \simeq \hat{F}_p\Phi(x,y). \tag{13}$$

Now, by using (5), (7), (8), (11)–(13), we get

$$\begin{aligned}
&\Phi^T(x,y)\hat{F}\\
&\simeq \Phi^T(x,y)G + \tfrac{1}{\Gamma(\iota_1)\Gamma(\iota_2)}\int_0^x\int_0^y (x-\tau)^{\iota_1-1}(y-\varsigma)^{\iota_2-1}\Phi^T(x,y)K\Phi(\tau,\varsigma)\\
&\quad\times\hat{F}_p\Phi(\tau,\varsigma)d\varsigma d\tau\\
&\simeq \Phi^T(x,y)G + \tfrac{1}{\Gamma(\iota_1)\Gamma(\iota_2)}\int_0^x\int_0^y (x-\tau)^{\iota_1-1}(y-\varsigma)^{\iota_2-1}\Phi^T(x,y)K\\
&\quad\times\tilde{\hat{F}}_p^T\Phi(\tau,\varsigma)d\varsigma d\tau\\
&= \Phi^T(x,y)G + \Phi^T(x,y)K\tilde{\hat{F}}_p^T\tfrac{1}{\Gamma(\iota_1)\Gamma(\iota_2)}\int_0^x\int_0^y (x-\tau)^{\iota_1-1}(y-\varsigma)^{\iota_2-1}\\
&\quad\times\Phi(\tau,\varsigma)d\varsigma d\tau\\
&\simeq \Phi^T(x,y)G + \Phi^T(x,y)K\tilde{\hat{F}}_p^T(\mathbf{I}^{\iota_1}\otimes\mathbf{I}^{\iota_2})\Phi(x,y).
\end{aligned}$$

So, we have

$$\Phi^T(x,y)\hat{F} \simeq \Phi^T(x,y)G + \Phi^T(x,y)K\tilde{\hat{F}}_p^T(\mathbf{I}^{\iota_1}\otimes\mathbf{I}^{\iota_2})\Phi(x,y). \tag{14}$$

To obtain unknown coefficients $\hat{f}_{ij}$, for $i,j = 0,1,\ldots,N$, in the above system, we choose an appropriate N and use the roots of $\mathscr{J}^{(\varrho,\vartheta)}_{\ell_1,N+1}(x)$ and $\mathscr{J}^{(\varrho,\vartheta)}_{\ell_2,N+1}(y)$. So we collocate Eq. (14) at $(N+1)^2$ points $\{(x_i,y_j)\}_{i,j=0}^N$. Therefore, we obtain $(N+1)^2$ algebraic equations and solve the arising nonlinear system by the Newton method. Then, from (5), we can determine an approximate solution for 2D-NFVIE for various values of ϱ and ϑ.

4.2. The method for 2D-NFFIEs

Now we want to convert Eq. (2) to a nonlinear system by using the two-variable SJPs. For this purpose, we apply (5), (7), (9)–(13) in (2) and therefore we obtain

$$\begin{aligned}
&\Phi^T(x,y)\hat{F} \simeq \Phi^T(x,y)G + \tfrac{1}{\Gamma(\iota_1)\Gamma(\iota_2)}\int_0^{\ell_1}\int_0^{\ell_2} (\ell_1-\tau)^{\iota_1-1}(\ell_2-\varsigma)^{\iota_2-1}\Phi^T(x,y)K\Phi(\tau,\varsigma)\\
&\quad\times\hat{F}_p\Phi(\tau,\varsigma)d\varsigma d\tau\\
&\simeq \Phi^T(x,y)G + \tfrac{1}{\Gamma(\iota_1)\Gamma(\iota_2)}\int_0^{\ell_1}\int_0^{\ell_2} (\ell_1-\tau)^{\iota_1-1}(\ell_2-\varsigma)^{\iota_2-1}\Phi^T(x,y)K\\
&\quad\times\tilde{\hat{F}}_p^T\Phi(\tau,\varsigma)d\varsigma d\tau\\
&= \Phi^T(x,y)G + \Phi^T(x,y)K\tilde{\hat{F}}_p^T\tfrac{1}{\Gamma(\iota_1)\Gamma(\iota_2)}\int_0^{\ell_1}\int_0^{\ell_2} (\ell_1-\tau)^{\iota_1-1}(\ell_2-\varsigma)^{\iota_2-1}\\
&\quad\times\Phi(\tau,\varsigma)d\varsigma d\tau\\
&\simeq \Phi^T(x,y)G + \Phi^T(x,y)K\tilde{\hat{F}}_p^T(Y_1\otimes Y_2).
\end{aligned}$$

So, we have

$$\Phi^T(x,y)\hat{F} \simeq \Phi^T(x,y)G + \Phi^T(x,y)K\tilde{\hat{F}}_p^T(Y_1\otimes Y_2). \tag{15}$$

Obtaining the unknown coefficients $\hat{f}_{ij}$ in the above system is similar to (14). Therefore we can determine an approximate solution for 2D-NFFIE from (5), for various values of ϱ and ϑ.

5. Error bound for the approximation

Let $\Omega = [0,\ell_1]\times[0,\ell_2]$ and the weighted space $L^2_{\omega^{(\varrho,\vartheta)}}(\Omega)$ be the space of square integrable functions in Ω. To verify the convergence of the presented method first we define the following inner product and norm on $L^2_{\omega^{(\varrho,\vartheta)}}(\Omega)$:

$$\langle f,g\rangle_{\omega^{(\varrho,\vartheta)}} = \int_0^{\ell_1}\int_0^{\ell_2} f(x,y)g(x,y)\omega^{(\varrho,\vartheta)}(x,y)\,dy\,dx, \qquad \forall f,g\in L^2_{\omega^{(\varrho,\vartheta)}}(\Omega),$$
$$\|f\|_{\omega^{(\varrho,\vartheta)}} = \left(\int_0^{\ell_1}\int_0^{\ell_2} (f(x,y))^2\omega^{(\varrho,\vartheta)}(x,y)\,dy\,dx\right)^{\frac{1}{2}}, \qquad \forall f\in L^2_{\omega^{(\varrho,\vartheta)}}(\Omega).$$

Theorem 3. *Let*

$$\mathscr{P}_N = span\left\{\mathscr{J}^{(\varrho,\vartheta)}_{ij}(x,y), \quad 0\leqslant i,j\leqslant N\right\},$$

be the finite-dimensional polynomial space. Suppose that

$$\frac{\partial^i g(x,y)}{\partial x^{i-j}\partial y^j}\in C(\Omega), \quad 0\leqslant i\leqslant N, 0\leqslant j\leqslant i.$$

If $g_N(x,y)$be the best approximate solution from N to $g(x,y)$ and $\tilde{g}_N(x,y)$ be the Taylor expansion of $g(x,y)$, then

$$\|g-g_N\|_{\omega^{(\varrho,\vartheta)}} \leqslant C_1(\ell_1\ell_2)^{\frac{\vartheta+\varrho+1}{2}}B(\varrho+1,\vartheta+1)\times\sum_{i=0}^{N+1}\frac{1}{(N+1-i)!i!}, \tag{16}$$

where

$$C_1 = \max_{0\leqslant i\leqslant N+1}\left\{\ell_1^{N+1-i}\ell_2^i\max_{(x,y)\in\Omega}\left|\frac{\partial^{N+1}g(\eta_x,\eta_y)}{\partial x^{N+1-i}\partial y^i}\right|\right\}, \tag{17}$$

and $(\eta_x,\eta_y)\in[0,x]\times[0,y]$.

Proof. By considering the Taylor expansion of gabout $(0^+,0^+)$, we have

$$\tilde{g}_N(x,y)=\sum_{i=0}^{N}\sum_{j=0}^{i}\frac{x^{i-j}y^j}{(i-j)!j!}\frac{\partial^i g(0^+,0^+)}{\partial x^{i-j}\partial y^j}.$$

Therefore, we obtain

$$\begin{aligned}\left|g(x,y)-\tilde{g}_N(x,y)\right| &= \left|g(x,y)-\sum_{i=0}^{N}\sum_{j=0}^{i}\frac{x^{i-j}y^j}{(i-j)!j!}\frac{\partial^i g(0^+,0^+)}{\partial x^{i-j}\partial y^j}\right| \\ &= \left|\sum_{i=0}^{N+1}\frac{x^{N+1-i}y^i}{(N+1-i)!i!}\frac{\partial^{N+1}g(\eta_x,\eta_y)}{\partial x^{N+1-i}\partial y^i}\right| \\ &\leqslant \sum_{i=0}^{N+1}\frac{x^{N+1-i}y^i}{(N+1-i)!i!}\left|\frac{\partial^{N+1}g(\eta_x,\eta_y)}{\partial x^{N+1-i}\partial y^i}\right| \\ &\leqslant \sum_{i=0}^{N+1}\frac{\ell_1^{N+1-i}\ell_2^i}{(N+1-i)!i!}\max_{(x,y)\in\Omega}\left|\frac{\partial^{N+1}g(\eta_x,\eta_y)}{\partial x^{N+1-i}\partial y^i}\right| \\ &\leqslant C_1\sum_{i=0}^{N+1}\frac{1}{(N+1-i)!i!},\end{aligned}$$

where $\left(\eta_x,\eta_y\right)\in[0,x]\times[0,y],(x,y)\in\Omega$, and C_1 is defined in (17). Since $g_N\in\mathscr{P}_N$ is the best approximation to g, we have

$$\begin{aligned}||g-g_N||^2_{\omega^{(\varrho,\vartheta)}} &\leqslant ||g-\tilde{g}_N||^2_{\omega^{(\varrho,\vartheta)}} \\ &= \int_0^{\ell_1}\int_0^{\ell_2}(g(x,y)-g^{\sim}{}_N(x,y))^2\omega^{(\varrho,\vartheta)}(x,y)\mathrm{d}y\mathrm{d}x \\ &\leqslant \left(C_1\sum_{i=0}^{N+1}\frac{1}{(N+1-i)!i!}\right)^2\int_0^{\ell_1}\int_0^{\ell_2}\omega^{(\varrho,\vartheta)}(x,y)\mathrm{d}y\mathrm{d}x \\ &= \left(C_1\sum_{i=0}^{N+1}\frac{1}{(N+1-i)!i!}\right)^2(\ell_1\ell_2)^{\vartheta+\varrho+1}(B(\varrho+1,\vartheta+1))^2\end{aligned}$$

Now we can take the square roots and therefore we conclude the proof of the theorem. □

Theorem 4. *Suppose that*

$$\frac{\partial^{i_1}k(x,y,\tau,\varsigma)}{\partial x^{i_1-i_2}\partial y^{i_2-i_3}\partial\tau^{i_3-i_4}\partial\varsigma^{i_4}}\in C(\Omega\times\Omega),$$

for $0\leqslant i_1\leqslant N, 0\leqslant i_2\leqslant i_1, 0\leqslant i_3\leqslant i_2, 0\leqslant i_4\leqslant i_3$.
If $k_N(x,y,\tau,\varsigma)$ *be the best approximate solution to* $k(x,y,\tau,\varsigma)$ *obtained by the proposed method and* $\tilde{k}_N(x,y,\tau,\varsigma)$ *be the Taylor expansion of* $k(x,y,\tau,\varsigma)$*, then*

$$\begin{aligned}||k-k_N||^2_{\omega^{(\varrho,\vartheta)}} &\leqslant C_2(\ell_1\ell_2)^{\vartheta+\varrho+1}(B(\varrho+1,\vartheta+1))^2 \\ &\times\sum_{i_1=0}^{N+1}\sum_{i_2=0}^{i_1}\sum_{i_3=0}^{i_2}\frac{1}{(N+1-i_1)!(i_1-i_2)!(i_2-i_3)!i_3!},\end{aligned}\tag{18}$$

where

$$\begin{aligned}C_2 = \max_{0\leqslant i_1,i_2,i_3\leqslant N+1}&\left\{\ell_1^{N+1-i_1+i_2-i_3}\ell_2^{i_1-i_2+i_3}\right. \\ &\left.\times\max_{(x,y,\tau,\varsigma)\in\Omega\times\Omega}\left|\frac{\partial^{N+1}k(\eta_x,\eta_y,\eta_\tau,\eta_\varsigma)}{\partial x^{N+1-i_1}\partial y^{i_1-i_2}\partial\tau^{i_2-i_3}\partial\varsigma^{i_3}}\right|\right\},\end{aligned}\tag{19}$$

and $\left(\eta_x,\eta_y,\eta_\tau,\eta_\varsigma\right)\in[0,x]\times[0,y]\times[0,\tau]\times[0,\varsigma]$.

Proof. By considering the Taylor expansion of $k(x,y,\tau,\varsigma)$about $(0^+,0^+,0^+,0^+)$, we have

$$\begin{aligned}\tilde{k}_N(x,y,\tau,\varsigma) = \sum_{i_1=0}^{N}\sum_{i_2=0}^{i_1}\sum_{i_3=0}^{i_2}\sum_{i_4=0}^{i_3}&\left(\frac{x^{i_1-i_2}y^{i_2-i_3}\tau^{i_3-i_4}\varsigma^{i_4}}{(i_1-i_2)!(i_2-i_3)!(i_3-i_4)!i_4!}\right. \\ &\left.\times\frac{\partial^{i_1}k(0^+,0^+,0^+,0^+)}{\partial x^{i_1-i_2}\partial y^{i_2-i_3}\partial\tau^{i_3-i_4}\partial\varsigma^{i_4}}\right).\end{aligned}$$

Therefore, we obtain

$$\begin{aligned}&\left|k(x,y,\tau,\varsigma)-\tilde{k}_N(x,y,\tau,\varsigma)\right| \\ &= \left|k(x,y,\tau,\varsigma)-\sum_{i_1=0}^{N}\sum_{i_2=0}^{i_1}\sum_{i_3=0}^{i_2}\sum_{i_4=0}^{i_3}\left(\frac{x^{i_1-i_2}y^{i_2-i_3}\tau^{i_3-i_4}\varsigma^{i_4}}{(i_1-i_2)!(i_2-i_3)!(i_3-i_4)!i_4!}\right.\right. \\ &\left.\left.\times\frac{\partial^{i_1}k(0^+,0^+,0^+,0^+)}{\partial x^{i_1-i_2}\partial y^{i_2-i_3}\partial\tau^{i_3-i_4}\partial\varsigma^{i_4}}\right)\right| \\ &= \left|\sum_{i_1=0}^{N+1}\sum_{i_2=0}^{i_1}\sum_{i_3=0}^{i_2}\left(\frac{x^{N+1-i_1}y^{i_1-i_2}\tau^{i_2-i_3}\varsigma^{i_3}}{(N+1-i_1)!(i_1-i_2)!(i_2-i_3)!i_3!}\right.\right. \\ &\left.\left.\times\frac{\partial^{i_1}k(\eta_x,\eta_y,\eta_\tau,\eta_\varsigma)}{\partial x^{i_1-i_2}\partial y^{i_2-i_3}\partial\tau^{i_3-i_4}\partial\varsigma^{i_4}}\right)\right| \\ &\leqslant \sum_{i_1=0}^{N+1}\sum_{i_2=0}^{i_1}\sum_{i_3=0}^{i_2}\left(\frac{x^{N+1-i_1}y^{i_1-i_2}\tau^{i_2-i_3}\varsigma^{i_3}}{(N+1-i_1)!(i_1-i_2)!(i_2-i_3)!i_3!}\right. \\ &\left.\times\left|\frac{\partial^{i_1}k(\eta_x,\eta_y,\eta_\tau,\eta_\varsigma)}{\partial x^{i_1-i_2}\partial y^{i_2-i_3}\partial\tau^{i_3-i_4}\partial\varsigma^{i_4}}\right|\right) \\ &\leqslant \sum_{i_1=0}^{N+1}\sum_{i_2=0}^{i_1}\sum_{i_3=0}^{i_2}\left(\frac{\ell_1^{N+1-i_1+i_2-i_3}\ell_2^{i_1-i_2+i_3}}{(N+1-i_1)!(i_1-i_2)!(i_2-i_3)!i_3!}\right. \\ &\left.\times\max_{(x,y,\tau,\varsigma)\in\Omega\times\Omega}\left|\frac{\partial^{i_1}k(\eta_x,\eta_y,\eta_\tau,\eta_\varsigma)}{\partial x^{i_1-i_2}\partial y^{i_2-i_3}\partial\tau^{i_3-i_4}\partial\varsigma^{i_4}}\right|\right) \\ &\leqslant C_2\sum_{i_1=0}^{N+1}\sum_{i_2=0}^{i_1}\sum_{i_3=0}^{i_2}\frac{1}{(N+1-i_1)!(i_1-i_2)!(i_2-i_3)!i_3!},\end{aligned}$$

where $\left(\eta_x,\eta_y,\eta_\tau,\eta_\varsigma\right)\in[0,x]\times[0,y]\times[0,\tau]\times[0,\varsigma]$, and C_2 is defined in (19). Since $k_N$is the best approximation to k, we have

$$\begin{aligned}&||k-k_N||^2_{\omega^{(\varrho,\vartheta)}}\leqslant||k-\tilde{k}_N||^2_{\omega^{(\varrho,\vartheta)}} \\ &= \int_0^{\ell_1}\int_0^{\ell_2}\int_0^{\ell_1}\int_0^{\ell_2}\left(k(x,y,\tau,\varsigma)-\tilde{k}_N(x,y,\tau,\varsigma)\right)^2\omega^{(\varrho,\vartheta)}(x,y) \\ &\times\omega^{(\varrho,\vartheta)}(\tau,\varsigma)\mathrm{d}y\mathrm{d}x\mathrm{d}\varsigma\mathrm{d}\tau \\ &\leqslant \left(C_2\sum_{i_1=0}^{N+1}\sum_{i_2=0}^{i_1}\sum_{i_3=0}^{i_2}\frac{1}{(N+1-i_1)!(i_1-i_2)!(i_2-i_3)!i_3!}\right)^2 \\ &\times\int_0^{\ell_1}\int_0^{\ell_2}\int_0^{\ell_1}\int_0^{\ell_2}\omega^{(\varrho,\vartheta)}(x,y)\omega^{(\varrho,\vartheta)}(\tau,\varsigma)\mathrm{d}y\mathrm{d}x\mathrm{d}\varsigma\mathrm{d}\tau \\ &= \left(C_2\sum_{i_1=0}^{N+1}\sum_{i_2=0}^{i_1}\sum_{i_3=0}^{i_2}\frac{1}{(N+1-i_1)!(i_1-i_2)!(i_2-i_3)!i_3!}\right)^2 \\ &\times(\ell_1\ell_2)^{2(\vartheta+\varrho+1)}(B(\varrho+1,\vartheta+1))^4.\end{aligned}$$

Now we can take the square roots and therefore the proof is completed. □

Theorem 5. *Let* $f\in C(\Omega)$ *be the exact solution of Eq. (2) and* f_N *be its approximate solution obtained by the presented method. Suppose that for* $(x,y)\in\Omega=[0,\ell_1]\times[0,\ell_2]$ *the following assumptions hold:*

(C1) $g\in C(\Omega)$ *and* $k\in C(\Omega\times\Omega)$,
(C2) *There exists a Lipschitz constant* L *such that* $\left|f^p(x,y)-f_N^p(x,y)\right|\leqslant L|f(x,y)-f_N(x,y)|$,
(C3) $\sup_{(x,y)\in\Omega}|f^p(x,y)|=b<\infty$,
(C4) $\sup_{(x,y,\tau,\varsigma)\in\Omega\times\Omega}|k(x,y,\tau,\varsigma)|=c<\infty$.

Then, there exist positive constants C_l, a_1, *and* a_2 *such that*

$$\begin{aligned}||f-f_N||^2_{\omega^{(\varrho,\vartheta)}}\leqslant&\frac{1}{\Gamma(\imath_1+1)\Gamma(\imath_2+1)-\ell_1^{\imath_1}\ell_2^{\imath_2}a_1}\left(\Gamma(\imath_1+1)\Gamma(\imath_2+1)C_1\right. \\ &\times(\ell_1\ell_2)^{\frac{\vartheta+\varrho+1}{2}}B(\varrho+1,\vartheta+1)\sum_{i=0}^{N+1}\frac{1}{(N+1-i)!i!}+\ell_1^{\imath_1}\ell_2^{\imath_2}(\ell_1\ell_2)^{\vartheta+\varrho+1} \\ &\left.\times a_2(B(\varrho+1,\vartheta+1))^2\sum_{i_1=0}^{N+1}\sum_{i_2=0}^{i_1}\sum_{i_3=0}^{i_2}\frac{1}{(N+1-i_1)!(i_1-i_2)!(i_2-i_3)!i_3!}\right).\end{aligned}\tag{20}$$

Proof. Considering the two-variable SJPs expansions of $f(x,y)$ and $k(x,y,\tau,\varsigma)$ leads to

$$|f(x,y)-f_N(x,y)| \leqslant |g(x,y)-g_N(x,y)| + \left|\frac{1}{\Gamma(\iota_1)\Gamma(\iota_2)}\int_0^{\ell_1}\int_0^{\ell_2}(\ell_1-\tau)^{\iota_1-1}(\ell_2-\varsigma)^{\iota_2-1}k(x,y,\tau,\varsigma)f^p(\tau,\varsigma) - k_N(x,y,\tau,\varsigma)f_N^p(\tau,\varsigma)\mathrm{d}\varsigma\mathrm{d}\tau\right|.$$

It is clear that

$$\begin{aligned} k(x,y,\tau,\varsigma)f^p(\tau,\varsigma) - k_N(x,y,\tau,\varsigma)f_N^p(\tau,\varsigma) &= k(x,y,\tau,\varsigma)\big(f^p(\tau,\varsigma)-f_N^p(\tau,\varsigma)\big) \\ &\quad + (k(x,y,\tau,\varsigma)-k_N(x,y,\tau,\varsigma))f_N^p(\tau,\varsigma). \end{aligned} \tag{21}$$

By using Eq. (21) and from assumptions $C1-C4$, we obtain

$$\begin{aligned} &|f(x,y)-f_N(x,y)| \\ &\leqslant |g(x,y)-g_N(x,y)| \\ &\quad + \left|\frac{1}{\Gamma(\iota_1)\Gamma(\iota_2)}\int_0^{\ell_1}\int_0^{\ell_2}(\ell_1-\tau)^{\iota_1-1}(\ell_2-\varsigma)^{\iota_2-1}\right. \\ &\quad \left.\times k(x,y,\tau,\varsigma)(f^p(\tau,\varsigma)-f_N^p(\tau,\varsigma)) + (k(x,y,\tau,\varsigma)-k_N(x,y,\tau,\varsigma))f_N^p(\tau,\varsigma))\mathrm{d}\varsigma\mathrm{d}\tau\right| \\ &\leqslant |g(x,y)-g_N(x,y)| \\ &\quad + \frac{1}{\Gamma(\iota_1)\Gamma(\iota_2)}\int_0^{\ell_1}\int_0^{\ell_2}(\ell_1-\tau)^{\iota_1-1}(\ell_2-\varsigma)^{\iota_2-1}(Lc|f(\tau,\varsigma)-f_N(\tau,\varsigma)| + b|k(x,y,\tau,\varsigma) \\ &\quad - k_N(x,y,\tau,\varsigma)|)\mathrm{d}\varsigma\mathrm{d}\tau. \end{aligned} \tag{22}$$

Now by using (16), (18), and taking $L^2_{\omega^{(\varrho,\vartheta)}}$-norm in (22), we have

$$\|f-f_N\|_{\omega^{(\varrho,\vartheta)}} \leqslant \|g-g_N\|_{\omega^{(\varrho,\vartheta)}} + \frac{\ell_1^{\iota_1}\ell_2^{\iota_2}}{\Gamma(\iota_1+1)\Gamma(\iota_2+1)}(Lc\|f-f_N\|_{\omega^{(\varrho,\vartheta)}} + b\|k-k_N\|_{\omega^{(\varrho,\vartheta)}}).$$

Simplifying the above relation yields

$$\begin{aligned} \|f-f_N\|_{\omega^{(\varrho,\vartheta)}} &\leqslant \frac{1}{\Gamma(\iota_1+1)\Gamma(\iota_2+1)-\ell_1^{\iota_1}\ell_2^{\iota_2}Lc}\Big(\Gamma(\iota_1+1)\Gamma(\iota_2+1)\|g-g_N\|_{\omega^{(\varrho,\vartheta)}} \\ &\quad + \ell_1^{\iota_1}\ell_2^{\iota_2}b\|k-k_N\|_{\omega^{(\varrho,\vartheta)}}\Big) \\ &\leqslant \frac{1}{\Gamma(\iota_1+1)\Gamma(\iota_2+1)-\ell_1^{\iota_1}\ell_2^{\iota_2}Lc}\Big(\Gamma(\iota_1+1)\Gamma(\iota_2+1)C_1(\ell_1\ell_2)^{\frac{\vartheta+\varrho+1}{2}}B(\varrho+1,\vartheta+1) \\ &\quad \times\sum_{i=0}^{N+1}\frac{1}{(N+1-i)!i!} + \ell_1^{\iota_1}\ell_2^{\iota_2}(\ell_1\ell_2)^{\vartheta+\varrho+1}bC_2(B(\varrho+1,\vartheta+1))^2 \\ &\quad \times\sum_{i_1=0}^{N+1}\sum_{i_2=0}^{i_1}\sum_{i_3=0}^{i_2}\frac{1}{(N+1-i_1)!(i_1-i_2)!(i_2-i_3)!i_3!}\Big). \end{aligned}$$

Setting $a_1 = Lc$ and $a_2 = bC_2$, we get (20) which completes the proof of the theorem. □

Remark 1. Obviously the right hand side of the inequality (20) tends to zero as $N\to\infty$, so $f-f_N\to 0$ and this proves convergence of the proposed method.

Remark 2. For the 2D-NFVIE, since $(x,y)\in\Omega$, we can use similar way which has been used in Theorem 5.

6. Illustrative examples

Here, three test examples are presented by using Maple 2018 software to examine numerical results of the proposed method. In all of this section, $\hat{n}$denotes the number of bases that used for solving these problems. To show the accuracy and computational efficiency of our method, we use

$$|f(x,y)-f_N(x,y)|,\quad N\in\mathbb{N},$$

and

$$MAE := \max_{i,j=0,1,\ldots,N}\{|f(x_i,y_j)-f_N(x_i,y_j)|\},$$

which are, respectively, the absolute errors in the solutions and the maximum absolute errors, where points $(x_i,y_j),\ i,j=0,1,\ldots,N$ are roots of two-variable SJPs in the domain $\Omega=[0,\ell_1]\times[0,\ell_2]$ for different values of ϱ and ϑ.

Also, graphs of maximum absolute errors are plotted by using

$$\max_{j=0,1,\ldots,N}\{|f(x,y_j)-f_N(x,y_j)|\},\qquad x\in[0,\ell_1],$$

where points $y_j,\ j=0,1,\ldots,N$ are roots of one-variable SJPs in the interval $[0,\ell_2]$.

Example 1. Consider the following 2D-NFFIEs studied by Najafalizadeh and Ezzati (2016):

$$f(x,y) = \frac{2362}{4725}xy + \frac{1}{\Gamma(\frac{7}{2})\Gamma(\frac{7}{2})}\int_0^1\int_0^1(1-\tau)^{\frac{5}{2}}(1-\varsigma)^{\frac{5}{2}}xy \times\sqrt{\varsigma}f(\tau,\varsigma)\mathrm{d}\varsigma\mathrm{d}\tau,$$

with the exact solution $f(x,y)=\frac{1}{2}xy$.

Tables 1 and 2, respectively, report the exact and approximate solutions and also absolute errors in the solutions at selected points in the domain $\Omega=[0,1]\times[0,1]$ with $N=2,3$ and $\varrho=\vartheta=0$. Also, Table 3 report the maximum absolute errors with $N=2$ and different values of ϱ and ϑ. From these tables, we see that by using $\hat{n}=(N+1)^2=16$ numbers of two-variable SJPs, we obtain more accurate results than the methods reported in Hesameddini and Shahbazi (2018), Maleknejad et al. (2020a) and Najafalizadeh and

Table 1
Exact and approximate solutions with $\varrho=\vartheta=0$ and different values of N for Example 1.

$x=y$	Exact solution	Present method		2D-HBPSLs method		2D-SLPOM method		2D-BPFs method	
		$N=2$, $\hat{n}=9$	$N=3$, $\hat{n}=16$	$N=2,M=2$, $\hat{n}=16$	$N=2,M=3$, $\hat{n}=36$	$N=64$, $\hat{n}=4225$	$N=128$, $\hat{n}=16641$	$m=64$, $\hat{n}=4096$	$m=128$, $\hat{n}=16384$
0	0.000	$-2.48030e-16$	$-2.19037e-16$	0.0000000	0.000	0	0	0.000203	0
0.1	0.005	0.00499999	0.005	0.00499998	0.005	0.0049789	0.0499965	0.00157	0.004587
0.2	0.020	0.0199999	0.02	0.0199999	0.020	0.0199693	0.0199989	0.021056	0.02054
0.3	0.045	0.0449999	0.045	0.0449998	0.045	0.0449485	0.0449988	0.040154	0.04328
0.4	0.080	0.0799998	0.08	0.0799996	0.080	0.0799275	0.0799980	0.086581	0.081564
0.5	0.125	0.125	0.125	0.124999	0.125	0.1249110	0.1249941	0.12058	0.126196
0.6	0.180	0.18	0.18	0.179999	0.180	0.1799068	0.1799840	0.17985	0.18346
0.7	0.245	0.244999	0.245	0.244999	0.245	0.2448798	0.2449730	0.23982	0.247982
0.8	0.320	0.319999	0.32	0.319999	0.320	0.3198459	0.3199785	0.323195	0.32120
0.9	0.405	0.404999	0.405	0.404998	0.405	0.4046765	0.4049762	0.03905	0.406365
Max error	0	$1.022850e-06$	$4.599127e-08$	$1.692071e-06$	$5.786662e-08$	$1.97e-4$	$3.21e-5$	$7.23e-3$	$2.88e-3$

Table 2
Absolute errors with $\varrho = \vartheta = 0$ and different values of N for Example 1.

$x = y$	Present method		2D-HBPSLs method		2D-BPFs method	
	$N = 2$ $\hat{n} = 9$	$N = 3$ $\hat{n} = 16$	$N = 2, M = 2$ $\hat{n} = 16$	$N = 2, M = 3$ $\hat{n} = 36$	$m = 16$ $\hat{n} = 256$	$m = 32$ $\hat{n} = 1024$
0	2.480297e – 16	2.190366e – 16	0	0	1.14e – 3	6.14e – 4
0.1	1.299190e – 08	5.311034e – 10	2.210053e – 08	6.886606e – 10	1.67e – 2	6.24e – 3
0.2	5.196759e – 08	2.124413e – 09	8.840210e – 08	2.754642e – 09	1.09e – 2	7.93e – 3
0.3	1.169271e – 07	4.779930e – 09	1.989047e – 07	6.197945e – 09	1.62e – 2	7.22e – 3
0.4	2.078704e – 07	8.497654e – 09	3.536084e – 07	1.101857e – 08	9.23e – 3	2.53e – 3
0.5	3.247975e – 07	1.327758e – 08	5.525131e – 07	1.721651e – 08	2.58e – 2	1.32e – 2
0.6	4.677083e – 07	1.911972e – 08	7.956189e – 07	2.479178e – 08	7.44e – 3	4.61e – 3
0.7	6.366030e – 07	2.602406e – 08	1.082926e – 06	3.374437e – 08	2.58e – 2	1.48e – 2
0.8	8.314815e – 07	3.399062e – 08	1.414434e – 06	4.407428e – 08	9.97e – 3	5.27e – 3
0.9	1.052344e – 06	4.301937e – 08	1.790143e – 06	5.578151e – 08	2.32e – 2	1.32e – 2

Table 3
Maximum absolute errors with $N = 2$ and different values of ϱ and ϑ for Example 1.

(ϱ, ϑ)	*MAE*	(ϱ, ϑ)	*MAE*
(0, 0)	1.022850e – 06	(1, 1)	3.411632e – 06
(1, 2)	6.430087e – 06	(2, 1)	1.932574e – 06
(2, 2)	4.048932e – 06	(3, 2)	2.650344e – 06

Ezzati (2016) that respectively used $\hat{n} = (N+1)^2 = 129^2 = 16641$ 2D-SLPOM, $\hat{n} = N^2M^2 = 36$ 2D-HBPSLs, and $\hat{n} = m^2 = 128^2 = 16384$ 2D-BPFs for solving this problem. Figs. 1 and 2 illustrate the efficiency and accuracy of our method.

Example 2. Consider the following 2D-NFVIEs studied by Najafalizadeh and Ezzati (2016):

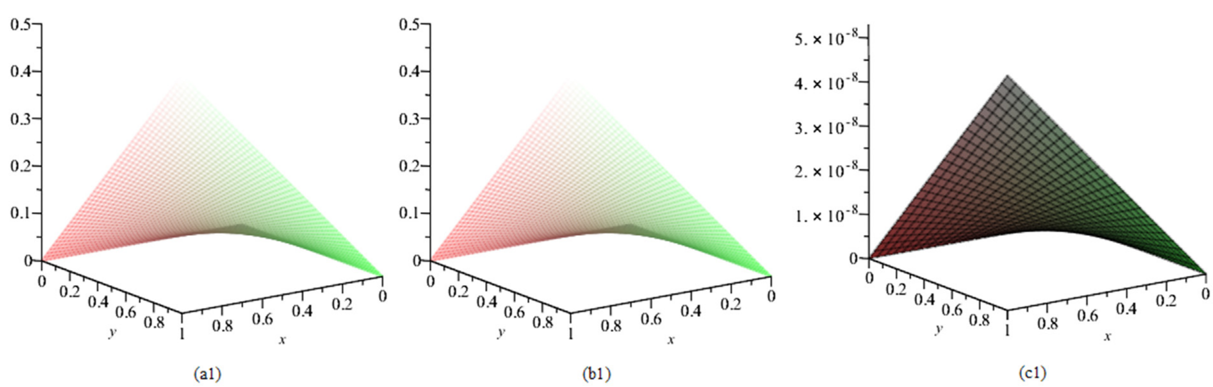

Fig. 1. Plots of: (a1) the exact solution, (b1) the approximate solution, (c1) the absolute error with $N = 3$ and $\varrho = \vartheta = 0$ for Example 1.

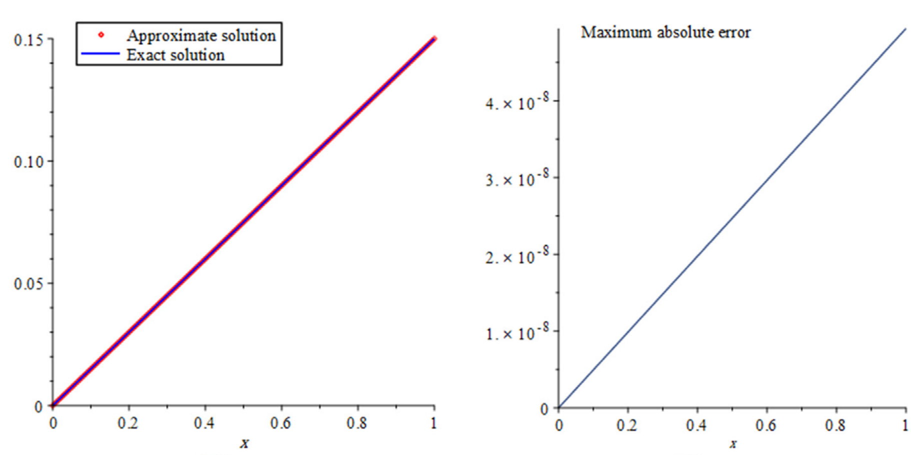

Fig. 2. Plots of: (d1) the comparison of the exact and approximate solutions, (e1) the maximum absolute error at $y = 0.3$ with $N = 3$ and $\varrho = \vartheta = 0$ for Example 1.

Table 4
Exact and approximate solutions with $\varrho = 1,\ \vartheta = 2$ and different values of N for Example 2.

$x = y$	Exact solution	Present method		2D-OBPs method		2D-BPFs method	
		$N = 2$ $\hat{n} = 9$	$N = 3$ $\hat{n} = 16$	$N = 3$ $\hat{n} = 16$	$N = 4$ $\hat{n} = 25$	$m = 16$ $\hat{n} = 256$	$m = 32$ $\hat{n} = 1024$
0	0	0.0331967	0.0200776	0.0205278	0.00848347	0.018452	0.009386
0.1	0.057735	0.0698879	0.0609538	0.0525517	0.0516175	0.031135	0.042121
0.2	0.115470	0.116196	0.113649	0.099356	0.114056	0.132610	0.124282
0.3	0.173205	0.169515	0.17175	0.160941	0.179512	0.147605	0.156905
0.4	0.230940	0.22743	0.231216	0.237306	0.235315	0.246768	0.239179
0.5	0.288675	0.287718	0.289899	0.296265	0.289476	0.262075	0.274574
0.6	0.346410	0.348347	0.347136	0.346426	0.346119	0.360925	0.354075
0.7	0.404145	0.407478	0.403441	0.400514	0.403987	0.378545	0.389848
0.8	0.461880	0.463463	0.460269	0.45853	0.462227	0.475083	0.468971
0.9	0.519615	0.514844	0.519876	0.520474	0.520042	0.501015	0.507021
Max error	0	2.165931e – 03	1.361947e – 03	1.285484e – 02	9.399035e – 03	2.96e – 02	1.63e – 02

Table 5
Absolute errors with $\varrho = 1,\ \vartheta = 2$ and different values of N for Example 2.

$x = y$	Present method		2D-OBPs method		2D-BPFs method	
	$N = 2$ $\hat{n} = 9$	$N = 3$ $\hat{n} = 16$	$N = 3$ $\hat{n} = 16$	$N = 4$ $\hat{n} = 25$	$N = 16$ $\hat{n} = 256$	$N = 32$ $\hat{n} = 1024$
0	3.319674e – 02	2.007764e – 02	4.08e – 2	1.69e – 2	1.84e – 2	9.38e – 3
0.1	1.215288e – 02	3.218750e – 03	1.15e – 2	4.78e – 3	2.66e – 2	1.56e – 2
0.2	7.259838e – 04	1.820797e – 03	1.03e – 2	1.22e – 2	1.71e – 2	8.81e – 3
0.3	3.690178e – 03	1.455357e – 03	2.50e – 2	1.01e – 2	2.56e – 2	1.63e – 2
0.4	3.510252e – 03	2.760137e – 04	3.23e – 2	2.82e – 3	1.57e – 2	8.23e – 3
0.5	9.573053e – 04	1.223501e – 03	3.23e – 2	5.85e – 3	2.66e – 2	1.41e – 2
0.6	1.937176e – 03	7.259284e – 04	2.49e – 2	1.24e – 2	1.45e – 2	7.66e – 3
0.7	3.333285e – 03	7.043849e – 04	1.03e – 2	1.38e – 2	2.56e – 2	1.42e – 2
0.8	1.582695e – 03	1.611293e – 03	1.16e – 2	7.41e – 3	1.32e – 2	7.09e – 3
0.9	4.771341e – 03	2.609636e – 04	4.09e – 2	8.99e – 3	1.86e – 2	1.25e – 2

Table 6
Maximum absolute errors with $N = 2$ and different values of ϱ and ϑ for Example 2.

(ϱ, ϑ)	*MAE*	(ϱ, ϑ)	*MAE*
(0, 0)	9.900443e – 03	(1, 1)	4.159019e – 03
(1, 2)	2.165931e – 03	(2, 1)	4.212117e – 03
(2, 2)	2.280892e – 03	(3, 2)	2.343278e – 03

$$f(x,y) = \sqrt{y}\left(-\frac{1}{180}x^3y^{\frac{7}{2}} + \sqrt{\frac{x}{3}}\right) + \frac{1}{\Gamma(\frac{3}{2})\Gamma(\frac{5}{2})}\int_0^x\int_0^y (x-\tau)^{\frac{1}{2}}(y-\varsigma)^{\frac{3}{2}} \times \sqrt{xy\varsigma}\, f^2(\tau,\varsigma)\,\mathrm{d}\varsigma\,\mathrm{d}\tau,$$

with the exact solution $f(x,y) = \frac{\sqrt{3xy}}{3}$.

Tables 4 and 5, respectively, report the exact and approximate solutions and also absolute errors in the solutions at selected points in the domain $\Omega = [0,1] \times [0,1]$ with $N = 2, 3$ and $\varrho = 1,\ \vartheta = 2$. Also, Table 6 report the maximum absolute errors with $N = 2$ and different values of ϱ and ϑ. From these tables, we see that by using $\hat{n} = (N+1)^2 = 16$ numbers of two-variable SJPs, we obtain more accurate results than the methods reported in Mirzaee and Samadyar (2019) and Najafalizadeh and Ezzati (2016) that respectively used $\hat{n} = (N+1)^2 = 25$ 2D-OBPs and $\hat{n} = m^2 = 32^2 = 1024$ 2D-BPFs for solving this problem. Figs. 3 and 4 illustrate the efficiency and accuracy of our method.

Example 3. Consider the following 2D-NFFIEs studied by Maleknejad et al. (2020a):

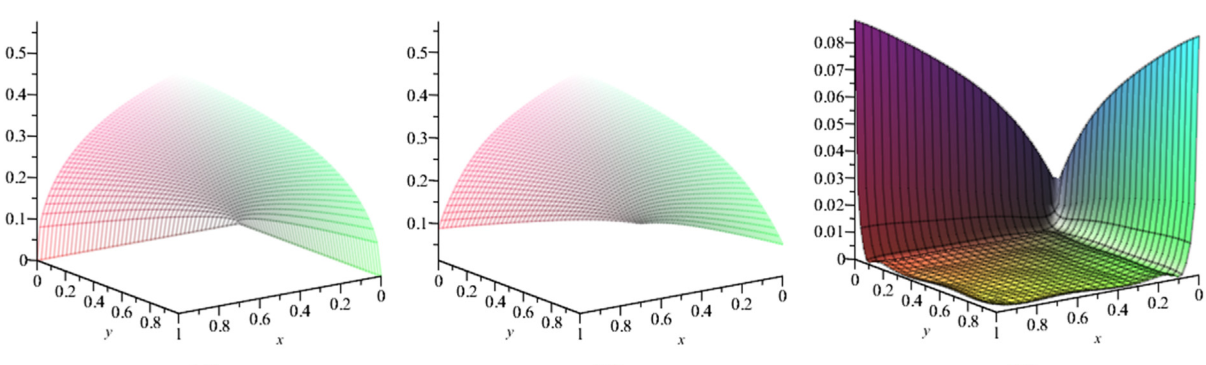

Fig. 3. Plots of: (a2) the exact solution, (b2) the approximate solution, (c2) the absolute error with $N = 4$ and $\varrho = 1,\ \vartheta = 2$ for Example 2.

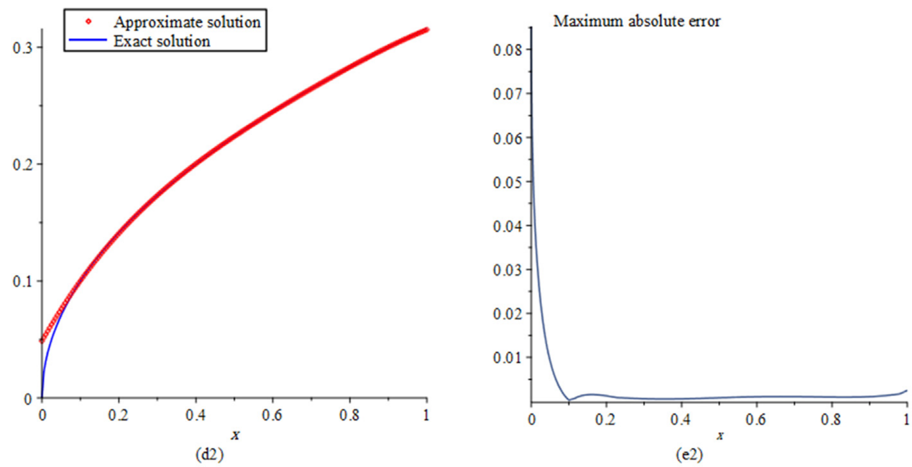

Fig. 4. Plots of: (d2) the comparison of the exact and approximate solutions, (e2) the maximum absolute error at $y = 0.3$ with $N = 4$ and $\varrho = 1,\ \vartheta = 2$ for Example 2.

Table 7
Exact and approximate solutions with $\varrho = \vartheta = 0$ and different values of N for Example 3.

$x = y$	Exact solution	Present method			2D-HBPSLs method		
		$N = 2$ $\hat{n} = 9$	$N = 3$ $\hat{n} = 16$	$N = 4$ $\hat{n} = 25$	$N = 2,\ M = 2$ $\hat{n} = 16$	$N = 2,\ M = 3$ $\hat{n} = 36$	$N = 2,\ M = 4$ $\hat{n} = 64$
0	0	0.00546634	−2.44588e − 05	8.62886e − 08	−0.00611009	7.16025e − 05	−2.11283e − 07
0.2	0.0618034	0.0684852	0.0640885	0.0616993	0.0596929	0.0636556	0.0620003
0.4	0.235114	0.246934	0.243635	0.235204	0.208992	0.237437	0.234909
0.6	0.48541	0.491344	0.489143	0.485647	0.441787	0.481357	0.485022
0.8	0.760845	0.752243	0.751142	0.76076	0.758077	0.755355	0.761687
1	1	0.980162	0.980162	0.99958	1.15907	1.01937	0.997307
1.2	1.14127	1.12563	1.12673	1.14114	1.14138	1.13298	1.14253
1.4	1.13262	1.13918	1.14138	1.13318	1.04019	1.12303	1.13172
1.6	0.940456	0.971338	0.974638	0.940817	0.855508	0.949467	0.939638
1.8	0.556231	0.572636	0.577033	0.555293	0.587328	0.572237	0.558005
Max error	0	3.520373e − 02	9.670138e − 04	8.015199e − 04	4.806815e − 02	1.238520e − 02	1.797677e − 03

Table 8
Absolute errors with $\varrho = \vartheta = 0$ and different values of N for Example 3.

$x = y$	Present method			2D-HBPSLs method		
	$N = 2$ $\hat{n} = 9$	$N = 3$ $\hat{n} = 16$	$N = 4$ $\hat{n} = 25$	$N = 2,\ M = 2$ $\hat{n} = 16$	$N = 2,\ M = 3$ $\hat{n} = 36$	$N = 2,\ M = 4$ $\hat{n} = 64$
0	5.466340e − 03	2.445883e − 05	8.628857e − 08	6.110089e − 03	7.160245e − 05	2.112827e − 07
0.2	6.681783e − 03	2.285147e − 03	1.041054e − 04	2.110473e − 03	1.852219e − 03	1.969093e − 04
0.4	1.182025e − 02	8.520440e − 03	9.018904e − 05	2.612231e − 02	2.323059e − 03	2.049089e − 04
0.6	5.933505e − 03	3.732523e − 03	2.364068e − 04	4.362368e − 02	4.053511e − 03	3.881470e − 04
0.8	8.602112e − 03	9.702936e − 03	8.517959e − 05	2.768116e − 03	5.490559e − 03	8.421973e − 04
1	1.983759e − 02	1.983759e − 02	4.204849e − 04	1.590742e − 01	1.937494e − 02	2.693277e − 03
1.2	1.563634e − 02	1.453551e − 02	1.278360e − 04	1.135362e − 04	8.291671e − 03	1.263460e − 03
1.4	6.556391e − 03	8.757374e − 03	5.514461e − 04	9.243113e − 02	9.597143e − 03	9.052617e − 04
1.6	3.088197e − 02	3.418178e − 02	3.604033e − 04	8.494829e − 02	9.010499e − 03	8.187792e − 04
1.8	1.640532e − 02	2.080196e − 02	9.377796e − 04	3.109712e − 02	1.600678e − 02	1.774201e − 03

$$f(x,y) = g(x,y) + \frac{1}{\Gamma(\frac{7}{2})\Gamma(1)} \int_0^2 \int_0^2 (2-\tau)^{\frac{5}{2}} \tau^2 \varsigma^{\frac{3}{2}} \cos\left(\frac{\pi}{2} y\right) f(\tau,\varsigma)\, d\varsigma\, d\tau,$$

where

$$g(x,y) = x \sin\left(\frac{\pi}{2} y\right) + \frac{32768\sqrt{2}\cos(\frac{\pi}{2} y)\left(-2\sqrt{2}\pi + 3\mathrm{FresnelS}\left(\sqrt{2}\right)\right)}{45045\pi^{\frac{5}{2}}}.$$

The exact solution of this equation is $f(x,y) = x\sin(\frac{\pi}{2} y)$. Note that $\mathrm{FresnelS}(x) = \int_0^x \sin\left(\frac{\pi t^2}{2}\right) dt$.

Tables 7 and 8, respectively, report the exact and approximate solutions and also absolute errors in the solutions at selected points in the domain $\Omega = [0,2] \times [0,2]$ with $N = 2,3,4$ and $\varrho = \vartheta = 0$. Also, Table 9 report the maximum absolute errors with

Table 9
Maximum absolute errors with $N = 2$ and different values of ϱ and ϑ for Example 3.

(ϱ, ϑ)	*MAE*	(ϱ, ϑ)	*MAE*
$(0,0)$	3.520373e − 02	$(\frac{1}{2}, \frac{1}{2})$	7.622338e − 02
$(\frac{1}{2}, -\frac{1}{2})$	4.889118e − 02	$(1,1)$	1.029894e − 01
$(1,2)$	1.413789e − 01	$(2,1)$	1.043501e − 01

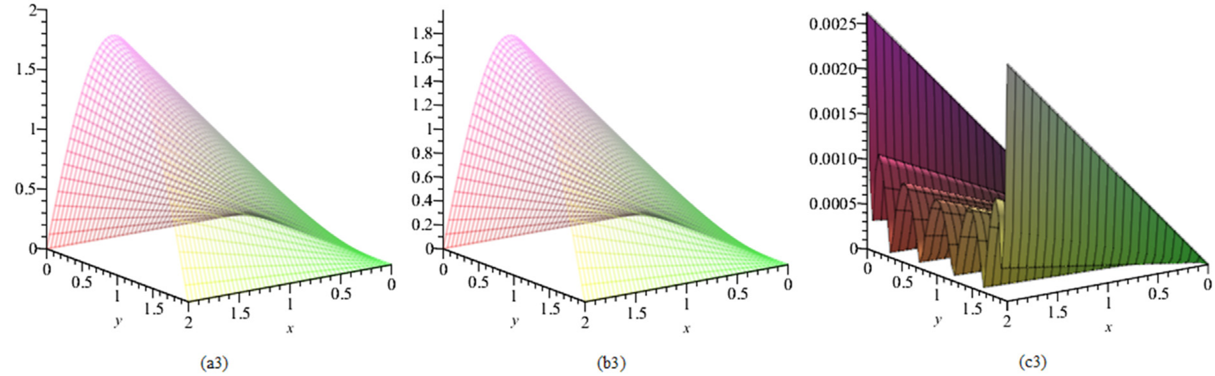

Fig. 5. Plots of: (a3) the exact solution, (b3) the approximate solution, (c3) the absolute error for $N = 4$ for Example 3.

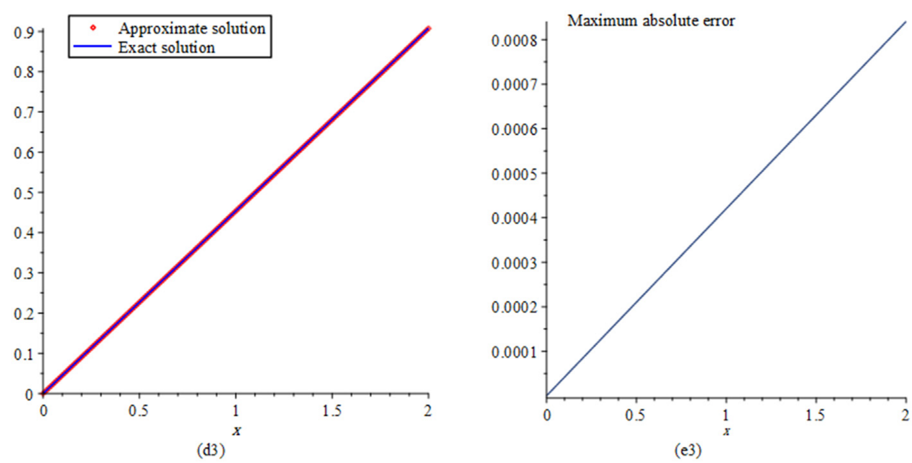

Fig. 6. Plots of: (d3) the comparison of the exact and approximate solutions, (e3) the maximum absolute error for $N = 4$ at $y = 0.3$ for Example 3.

$N = 2$ and different values of $\varrho$and ϑ. From these tables, we see that by using $\hat{n} = (N+1)^2 = 25$ numbers of two-variable SJPs, we obtain more accurate results than the method reported in Maleknejad et al. (2020a) that used $\hat{n} = N^2M^2 = 64$ 2D-HBPSLs for solving this problem. Figs. 5 and 6 illustrate the efficiency and accuracy of our method.

7. Conclusion

In this paper, we derived new operational matrices of fractional-order integration and product based on two-variable shifted Jacobi polynomials. These operational matrices utilized for solving the two-dimensional nonlinear fractional Fredholm and Volterra integral equations. Also, the error bound and convergence analysis for the proposed method were discussed. Moreover, the proposed method was evaluated by solving three numerical examples. Throughout the experimental examples, one can observe that the small size of operational matrices and basis functions are required to obtain a favorable approximate solution. The operational matrices obtained in this paper can be useful for numerically solving problems involving the left-sided mixed Riemann–Liouville integral operator of fractional order.

Declaration of Competing Interest

The authors declare that they have no known competing financial interests or personal relationships that could have appeared to influence the work reported in this paper.

References

Abbas, S., Benchohra, M., 2014. Fractional order integral equations of two independent variables. Applied Mathematics and Computation 227, 755–761.

Alkan, S., 2015. A new solution method for nonlinear fractional integro-differential equations. American Institute of Mathematical Sciences 8 (6), 1065–1077.

Atangana, A., Kílíçman, A., 2013a. Analytical solutions of the spacetime fractional derivative of advection dispersion equation. Mathematical Problems in Engineering 2013, 9. https://doi.org/10.1155/2013/853127.

Atangana, A., Kílíçman, A., 2013b. A possible generalization of acoustic wave equation using the concept of perturbed derivative order. Mathematical Problems in Engineering 2013, 6. https://doi.org/10.1155/2013/696597.

Benson, D.A., Wheatcraft, S.W., Meerschaert, M.M., 2000. Application of a fractional advection-dispersion equation. Water Resources Research 36 (6), 1403–1412.

Borhanifar, A., Sadri, Kh., 2016. A generalized operational method for solving integro-partial differential equations based on Jacobi polynomials. Hacettepe Journal of Mathematics and Statistics 45 (2), 311–335.

Caputo, M., 1967. Linear models of dissipation whose Q is almost frequency independent-part II. Geophysical Journal International 13 (5), 529–539.

Carpinteri, A., Mainardi, F., 1997. Fractals and Fractional Calculus in Continuum Mechanics. Springer-Verlag, New York, pp. 223–276.

Chen, C.M., Liu, F., Turner, I., Anh, V., 2007. A Fourier method for the fractional diffusion equation describing sub-diffusion. Journal of Computational Physics 227 (2), 886–897.

Cloot, A., Botha, J.F., 2006. A generalised groundwater flow equation using the concept of non-integer order derivatives. Water SA 32 (1), 55–78.

Hesameddini, E., Shahbazi, M., 2018. Two-dimensional shifted Legendre polynomials operational matrix method for solving the two-dimensional integral equations of fractional order. Applied Mathematics and Computation 322, 40–54.

Jabari Sabeg, D., Ezzati, R., Maleknejad, K., 2017. A new operational matrix for solving two-dimensional nonlinear integral equations of fractional order. Cogent Mathematics 4 (1), 1347017. https://doi.org/10.1080/23311835.2017.1347017.

Khalil, H., Khan, R.A., 2014. The use of Jacobi polynomials in the numerical solution of coupled system of fractional differential equations, International Journal of Computer Mathematics, doi: 10.1080/00207160.2014.945919..

Kumar, D., Singh, A.K., Sarveshanand, Mr, 2017. Effect of Hall current and wall conductance on hydromagnetic natural convection flow between vertical walls. International Journal of Industrial Mathematics. 9 (4), 289–299.
Kumar, D., Singh, A.K., Kumar, D., 2018. Effect of Hall current on the magnetohydrodynamic free convective flow between vertical walls with induced magnetic field. European Physical Journal Plus 133, 207. https://doi.org/10.1140/epjp/i2018-12012-4.
Kumar, D., Singh, A.K., Kumar, D., 2020. Influence of heat source/sink on MHD flow between vertical alternate conducting walls with Hall effect. Physica A 544,. https://doi.org/10.1016/j.physa.2019.123562 123562.
Ma, X., Huang, C., 2013. Numerical solution of fractional integro-differential equations by a hybrid collocation method. Applied Mathematics and Computation 219, 6750–6760.
Mainardi, F., 1997. Fractional calculus: Some basic problems in continuum and statistical mechanics. In: Carpinteri, A., Mainardi, F. (Eds.), Fractals and Fractional Calculus in Continuum Mechanics. Springer, New York, pp. 291–348.
Maleknejad, K., Rashidinia, J., Eftekhari, T., 2018. Numerical solution of three-dimensional Volterra-Fredholm integral equations of the first and second kinds based on Bernstein's approximation. Applied Mathematics and Computation 339, 272–285.
Maleknejad, K., Rashidinia, J., Eftekhari, T., 2020a. Operational matrices based on hybrid functions for solving general nonlinear two-dimensional fractional integro-differential equations. Computational and Applied Mathematics 39 (2), 1–34. https://doi.org/10.1007/s40314-020-1126-8.
Maleknejad, K., Rashidinia, J., Eftekhari, T., 2020b. Existence, uniqueness, and numerical solutions for two-dimensional nonlinear fractional Volterra and Fredholm integral equations in a Banach space. Computational and Applied Mathematics 39 (4), 1–22. https://doi.org/10.1007/s40314-020-01322-4.
Maleknejad, K., Rashidinia, J., Eftekhari, T., 2021. Numerical solutions of distributed order fractional differential equations in the time domain using the Müntz-Legendre wavelets approach. Numer Methods Partial Differential Eq. 37 (1), 707–731. https://doi.org/10.1002/num.22548.
Meerschaert, M.M., Tadjeran, C., 2004. Finite difference approximations for fractional advection-dispersion flow equations. Journal of Computational and Applied Mathematics 172 (1), 65–77.
Metzler, F., Schick, W., Kilian, H.G., Nonnenmacher, T.F., 1995. Relaxation in filled polymers: A fractional calculus approach. Journal of Chemical Physics 103, 7180–7186.
Mirzaee, F., Alipour, S., 2018. Numerical solution of nonlinear partial quadratic integro-differential equations of fractional order via hybrid of block-pulse and parabolic functions. Numerical Methods for Partial Differential Equations 35 (3), 1134–1151.
Mirzaee, F., Alipour, S., 2019a. Solving two-dimensional nonlinear quadratic integral equations of fractional order via operational matrix method. Multidiscipline Modeling in Materials and Structures 15 (6), 1136–1151.
Mirzaee, F., Alipour, S., 2019b. Fractional-order orthogonal Bernstein polynomials for numerical solution of nonlinear fractional partial Volterra integro-differential equations. Mathematical Methods in the Applied Sciences 42 (6), 1870–1893.
Mirzaee, F., Samadyar, N., 2018a. Convergence of 2D-orthonormal Bernstein collocation method for solving 2D-mixed Volterra-Fredholm integral equations. Transactions of A. Razmadze Mathematical Institute 172 (3), 631–641.
Mirzaee, F., Samadyar, N., 2018b. Application of hat basis functions for solving two-dimensional stochastic fractional integral equations. Computational and Applied Mathematics 37 (4), 4899–4916.
Mirzaee, F., Samadyar, N., 2019. Numerical solution based on two-dimensional orthonormal Bernstein polynomials for solving some classes of two-dimensional nonlinear integral equations of fractional order. Applied Mathematics and Computation 344–345, 191–203.
Mirzaee, F., Alipour, S., Samadyar, N., 2018. A numerical approach for solving weakly singular partial integro-differential equations via two-dimensional-orthonormal Bernstein polynomials with the convergence analysis. Numerical Methods for Partial Differential Equations 35 (2), 615–637.
Maleknejad, K., Rashidinia, J., Eftekhari, T., 2020. A new and efficient numerical method based on shifted fractional-order Jacobi operational matrices for solving some classes of two-dimensional nonlinear fractional integral equations, submitted to Numer Methods Partial Differential Eq.
Mohammed, D. Sh., 2014. Numerical solution of fractional integro-differential equations by least squares method and shifted Chebyshev polynomial. Mathematical Problems in Engineering, 2014, Article ID 431965, 5 pages. doi: 10.1155/2014/431965..
Najafalizadeh, S., Ezzati, R., 2016. Numerical methods for solving two-dimensional nonlinear integral equations of fractional order by using two-dimensional block pulse operational matrix. Applied Mathematics and Computation 280, 46–56.
Nemati, S., Lima, P.M., Sedaghat, S., 2020. Legendre wavelet collocation method combined with the Gauss-Jacobi quadrature for solving fractional delay-type integro-differential equations. Applied Numerical Mathematics 149, 99–112.
Oldham, K.B., Spanier, J., 1974. The Fractional Calculus. Academic Press, New York, London.
Podlubony, I., 1999. Fractional Differential Equations. Academic Press, San Diego.
Samadyar, N., Mirzaee, F., 2019. Numerical scheme for solving singular fractional partial integro-differential equation via orthonormal Bernoulli polynomials. International Journal of Numerical Modelling 32, (6) e2652.
Singh, H., 2020a. Analysis for fractional dynamics of Ebola virus model. Chaos Solitons & fractals 138, 109992.
Singh, H., 2020b. Numerical simulation for fractional delay differential equations. International Journal of Dynamic and Control. https://doi.org/10.1007/s40435-020-00671-6.
Singh, H., Srivastava, H.M., 2020. Numerical Simulation for Fractional-Order Bloch Equation Arising in Nuclear Magnetic Resonance by Using the Jacobi Polynomials. Applied Science 10, 2850.
Singh, H., Pandey, R.K., Srivastava, H.M., 2019. Solving non-linear fractional variational problems using Jacobi polynomials. Mathematics 7, 224.
Singh, H., Akhavan Ghassabzadeh, F., Tohidi, E., Cattani, Carlo, 2020. Legendre spectral method for the fractional Bratu problem. Mathematical Methods in the Applied Sciences 43 (9), 5941–5952. https://doi.org/10.1002/mma.6334.
Thomas, R., Fehmi, C., 2010. An immersed finite element method with integral equation correction. International Journal for Numerical Methods in Engineering 86, 93–114.
Yadav, S., Kumar, D., Singh, A.K., 2019. Magnetohydrodynamic flow in horizontal concentric cylinders. International Journal of Industrial Mathematics 11 (2), 89–98.
Yuste, S.B., Acedo, L., 2005. An explicit finite difference method and a new von Neumann-type stability analysis for fractional diffusion equations. SIAM Journal on Numerical Analysis 42 (5), 1862–1874.
Zhuang, P., Liu, F., Anh, V., Turner, I., 2009. Numerical methods for the variable-order fractional advection-diffusion equation with a nonlinear source term. SIAM Journal on Numerical Analysis 47, 1760–1781.